



Extension of the measurement range of electrical conductivity by time-domain reflectometry (TDR)

M.A. Mojid¹, G.C.L. Wyseure² and D.A. Rose*

Department of Agricultural and Environmental Science, University of Newcastle, Newcastle upon Tyne NE1 7RU, UK.

¹ Department of Irrigation and Water Management, Bangladesh Agricultural University, Mymensingh 2202, Bangladesh.

² Faculty of Agricultural and Applied Biological Sciences, K.U. Leuven, Kardinaal Mercierlaan 92, B-3001, Leuven, Belgium.

* Corresponding author.

Abstract

The electrical conductivity (EC) of a medium invaded by TDR sensors can be estimated from the impedance of a TDR reflectogram. Four categories of sensor were tested in salt solutions and the impedances of the TDR pulse wave were correlated to the EC of the solution. The relation between the impedance and EC over a wide range of conductivities is non-linear but stable. Second- to fourth-degree polynomials can extend the measurement range to 44 dS m^{-1} (equivalent to a NaCl concentration of 28 g l^{-1} or 0.48 N) and result in better prediction of the conductivities than linear relations. For automatic measurement of EC with a datalogger, the method of Giese and Tiemann (1975, *Adv. Mol. Rel. Processes*, 7: 45–59) gives accurate measurement of conductivities lower than 10 dS m^{-1} . Polynomial relations between EC and the datalogger's record provide an accurate estimate of the conductivity over a wide range. However, for both manual and automatic measurements, the sensors need to be calibrated individually. In particular, in the non-linear region, the differences between sensors are larger. Fortunately, the relation is sufficiently stable to eliminate significant error.

Introduction

Time-domain reflectometry (TDR) is an established method for measuring the volumetric water content of soils. It also has the potential to measure the electrical conductivity (EC) of solutions and soils. The electrical conductivity of soils enables the calculation of the concentration of solute in soil water, which can be used to construct solute-breakthrough curves to determine solute-transport parameters (Mallants *et al.*, 1994; Ward *et al.*, 1994, 1995; Vanclooster *et al.*, 1995; Mojid, 1996; Vogeler *et al.*, 1996). The success or failure of the TDR technique for these measurements depends on the accuracy of the calibration involved (Mallants *et al.*, 1996). However, it is claimed that the electrical conductivity of a bulk soil can only be measured for soil-water electrical conductivity up to 8 or 10 dS m^{-1} (Dalton, 1992; Van-clooster *et al.*, 1993) or up to 14 to 20 dS m^{-1} (Dalton and van Genuchten, 1986). Most references express the electrical conductivity of bulk soil in relation to the electrical conductivity of soil water, whereas TDR measures the electrical conductivity of bulk soil, termed the *bulk electrical conductivity*. Dalton and van Genuchten (1986)

claimed a proportional attenuation of the amplitude of the reflected voltage pulse with EC. They found close agreement between the electrical conductivities measured by TDR and by four-probe techniques, both measuring bulk EC. Kachanoski *et al.* (1992) developed a relationship between the attenuation of the TDR signal and the EC of the bulk soil. Dalton *et al.* (1984), Topp *et al.* (1988), Yanuka *et al.* (1988) and Zegelin *et al.* (1989) independently suggested theoretical approaches (Table 1) to determine electrical conductivities from the amplitudes of the TDR wave. In these equations, σ is the electrical conductivity of the medium (S m^{-1}), ϵ is the dielectric constant of the medium, L_s is the length of the sensor (m), and V_0 , V_1 , V_2 and V_f are the impedances (Ω) of the TDR trace (Fig. 1).

Unfortunately, the electrical conductivities estimated in the present study by these methods deviate considerably from each other (Nadler *et al.*, 1991) as illustrated by an example in Table 1. These methods also do not apply over a wide range of conductivities (Nadler *et al.*, 1991). Dalton *et al.* (1984) and Dalton and van Genuchten (1986) ignored the effects of multiple

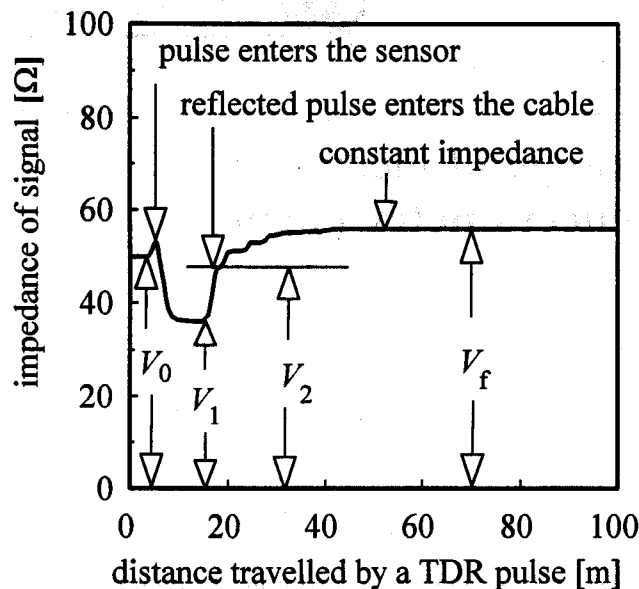


Fig. 1 A typical display of the TDR reflectogram in water.

reflections of the signal, caused by the discontinuities of the impedance, from the entrance and end of the sensor. To overcome these multi-reflection interferences, Topp *et al.* (1988), Yanuka *et al.* (1988), Zegelin *et al.* (1989) and Nadler *et al.* (1991) suggested using the impedance at a longer distance on the horizontal axis of the TDR reflectogram to determine the EC. Nadler *et al.* (1991) proposed a linear relation between the bulk EC and the impedance after multiple reflections. They included a probe constant and defined it in terms of the length and characteristic impedance of the sensor. Vanclooster *et al.* (1993) also claimed a linear relation between the bulk EC of the soil and the ratio of the impedance of the ingoing signal to the impedance of the signal after multiple reflections. However, the actual relation between the electrical conductivity, σ , and the impedance after multiple reflections, V_f , is non-linear (Heimovaara, 1993; Vanclooster *et al.*, 1994; Ward *et al.*, 1994). The non-linearity increases with increasing conductivity. The characteristics of the sensor also influence the non-

linearity. Heimovaara (1993) suggested subtracting the combined series resistance, R_{cs} (Ω), of the cable, connectors and TDR instrument, from the impedance after multiple reflections to compensate for the non-linearity at higher conductivities. The mathematical expression is:

$$\sigma = K_c / (V_f - R_{cs}) \quad (1)$$

where σ is the electrical conductivity ($S\ m^{-1}$) and K_c is a probe constant (m^{-1}).

Recently, the components of the Campbell Scientific TDR system have been designed to apply TDR for measuring the EC of bulk soils and solutions. The mathematical relation of Giese and Tiemann (1975), described in the next section, is used in an EPROM-program. The conductivity of the medium surrounding a TDR sensor attenuates the signal rapidly, and limits the measurement of electrical conductivity as well as soil-water content. Dalton and van Genuchten (1986) and Dalton (1992) could measure the bulk EC of soils for pore-water electrical conductivities of less than 14–20 $dS\ m^{-1}$, depending on the soil-water content. Zegelin *et al.* (1989) noted rapid attenuation of the TDR signal in highly conductive media and observed a greater influence of the conductivity on two-wire sensors than on three-wire sensors. They measured reflected signals at 20 °C in a series of aqueous solutions of sodium chloride (NaCl) whose concentrations varied from 0–2.9 $g\ l^{-1}$. They observed a complete attenuation of the reflected signal at 1 $dS\ m^{-1}$ for the two-wire sensors compared to 6 $dS\ m^{-1}$ for the three-wire sensors. In both cases, the length of the sensor was 15 cm. In their experiments, the three-wire sensors and the coaxial cell measured identical electrical conductivities but the two-wire sensors measured substantially different values for the same solutions. Zegelin *et al.* (1989) concluded that three-wire sensors were superior to two-wire sensors.

Theory of measuring electrical conductivity by TDR

The ordinate of a TDR reflectogram (Fig. 1) displays the impedance of the pulse wave which is proportional to the

Table 1. Theoretical equations for determining bulk electrical conductivity from a TDR wave form with an example of their performance (example has $\epsilon = 86$ (TDR-measured higher ϵ in saline water), $L_s = 0.15\ m$, $V_0 = 50\ \Omega$, $V_1 = 12.2\ \Omega$, $V_2 = 19.4\ \Omega$ and $V_f = 17.3\ \Omega$)

Equation	Source	EC ($dS\ m^{-1}$)	
		Estimated	Actual
$\sigma = (\sqrt{\epsilon} / 120\pi L_s) \ln [V_1 / (V_2 - V_1)]$	Dalton <i>et al.</i> , 1984	0.865	
$\sigma = (\sqrt{\epsilon} / 120\pi L_s) \ln \{V_1(2V_0 - V_1) / [V_0(V_2 - V_1)]\}$	Topp <i>et al.</i> , 1988	1.788	1.724
$\sigma = (\sqrt{\epsilon} / 120\pi L_s) \ln \{[V_1 V_f - V_0(V_1 + V_0)] / [V_0(V_1 - V_0)]\}$	Yanuka <i>et al.</i> , 1988	2.625	
$\sigma = (\sqrt{\epsilon} / 120\pi L_s) (V_1 / V_0) [(2V_0 - V_0) / (2V_0 - V_1)]$	Zegelin <i>et al.</i> , 1989	1.089	

energy of the generated signal. The attenuation of this energy depends on the conductivity of the medium through which the wave propagates. At a very long distance along the TDR trace, all reflections are suppressed. The impedance of the signal approaches a constant value for a given EC of the medium. This is equivalent to the impedance (resistance) of the direct-current component only. This impedance is independent of the characteristics of the transmission line, that is, the configuration, transfer-efficiency of the pulse, or multiple reflections (Nadler *et al.*, 1991; Kraus, 1992, p. 529). The dependency of the amplitude of the reflected signal on the conductivity of the medium is the basis of measuring EC by TDR. However, the exact interpretation of the signal for this purpose still remains controversial and is a topic of current research for many investigators. The method of Giese and Tiemann (1975) is used for the automatic measurement of the bulk EC with a datalogger. The mathematical expression of this method is:

$$\sigma = \frac{K_p}{Z} \frac{1 - \rho_r}{1 + \rho_r} \quad (2)$$

where σ is the bulk electrical conductivity ($S\ m^{-1}$), K_p is a probe constant (m^{-1}) for the method of Giese and Tiemann, Z is the impedance of the cable ($50\ \Omega$ for a coaxial cable), and ρ_r is a voltage reflection coefficient which is the ratio of the reflected voltage to the launched voltage.

Design and construction of TDR sensors

Parallel three-wire sensors were chosen in preference to two-wire sensors because of their better performance, especially under saline conditions. Four categories of sensor were constructed. Their geometry is described in Table 2. The design features of a parallel three-wire sensor are depicted in Figure 2. The wires of the sensor are connected to a coaxial cable of $50\ \Omega$ impedance with a quick transition, i.e. the transition between the coaxial cable and the wires in contact with the soil is as short as possible, to minimise any possible impedance mismatch

between the head of the sensor and the soil. Phenolic Fabric (brand name Tufnol), a material with good mechanical and electrical properties under dry and wet conditions, is used for the transition between the coaxial cable and the wires. Tufnol plate, 1 cm thick, keeps the stainless-steel rods (the wires of the sensor) parallel. A 5-mm groove is cut in the plate, through which the cable is connected. Precise holes are drilled in the plates so that only 5 mm of the wires are in the plate. The designed length (0.15 m) remains outside and will be in contact with the soil. A second plate is screwed onto the first plate. The two plates are glued together to make the head of the sensor waterproof. The grooves inside the heads of the second-type sensors were filled with commercial silicone sealant (usually semi-solid but becoming solid after drying) to make them stable and watertight. This also allows easy repair and maintenance of the sensors. The first and second types of sensor are virtually the same except that the second type contains silicone inside the head. The silicone dramatically changes the characteristics of the second-type sensors. To confirm the effects of the silicone, these sensors were tested again after removing the silicone from the heads.

Test of sensors in salt solutions

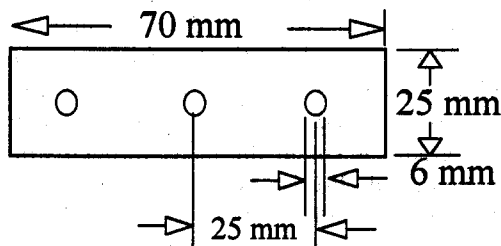
The TDR sensors were tested in solutions of sodium chloride. The objective was to correlate the impedances of the TDR wave with the electrical conductivities of the solutions. Three experiments (1, 2 & 3 in Table 3) were conducted for manual measurements and one (4 in Table 3) for automatic measurement. The type and number of the sensors used in each experiment are summarised in Table 3.

A PVC cylinder, 20 cm in diameter and 40 cm high with the base closed, was filled with distilled water. One sensor was immersed vertically and centrally into the water of the cylinder from a support at the top. The coaxial cable of the sensor was connected to a TDR (Tektronix 1502C). The TDR displays the reflected wave (Fig. 1) on the monitor. The impedances of the reflected wave were recorded at three locations (50, 100, and 624 m) on the reflectogram after multiple reflections. This

Table 2. Specifications and geometry of the four different types of sensor

Type of sensor	Length of rod (mm)	Diameter of rod (mm)	Spacing of rod (mm)	Length of cable (m)	Impedance of cable (Ω)
1	150	6	25	5.00	50
2	150	6	25	5.00	50
3	150	6	25	2.15	50
4	300	6	25	2.50	50

(a) Plan



(b) Elevation

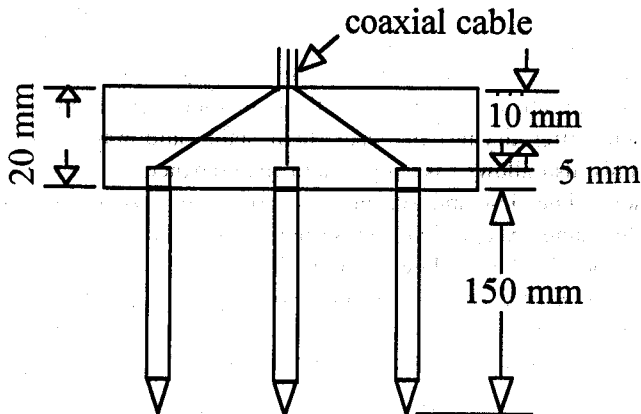


Fig. 2 A schematic diagram of the design of a parallel three-wire sensor.

was necessary because the impedance of the pulse signal increases rapidly over smaller distances and gradually becomes constant and equal to the resistance of the direct current after 6 to 7 bounces, that is, after 6 to 7 complete trips (Kraus, 1992, p. 527). This implies that, beyond a distance of 6 to 7 times the length of the wires of the sensor on the TDR trace, the impedance should be constant. But, in practice with TDR, the impedance changes with distance (it increases at lower conductivities but decreases at higher conductivities) gradually but slowly beyond this distance on the horizontal axis. At very high conductivities, an anomaly in the impedance is observed in the furthest section of the wave form. Up to a certain distance in the furthest section of the wave form, the impedance remains higher than the previous section. These anomalies depend on the characteristics of the specific sensor. Ward *et al.* (1994) also observed this type of anomaly. Therefore, the impedances at the three

Table 3. Type and number of sensors used in calibration tests

Experiment no.	Type 1	Type 2	Type 3	Type 4
1	2	—	2	1
2	1	7	—	—
3	3	4	—	—
4	3	5	—	—

different locations were used to evaluate the effects of the change of impedance with distance on the measurement of EC. All sensors were scanned in the same way one after another in the same cylinder of water. A sample of water was collected from the cylinder. Salt solution (NaCl) was added stepwise to the water in the cylinder and mixed thoroughly to increase its conductivity. All measurements and sampling were repeated. In this way, the conductivity was gradually increased up to 44 dS m^{-1} (i.e. up to a corresponding NaCl concentration of approximately $28 \text{ g l}^{-1} = 0.48 \text{ N}$) over 36 steps. For each conductivity level, the impedances of the signal were recorded for all sensors and a sample of solution was collected. However, for sensor type 4, the whole of the reflected signal was attenuated at about 22 dS m^{-1} (14 g l^{-1}). The temperature of the salt solution was also recorded at each step. The electrical conductivities of the solution samples were measured by a conductivity bridge at a reference temperature of 25°C . These were converted to the corresponding temperature at which the impedances were measured. The conversion is based on an increase (or decrease) of the conductivity by 2% of its measured value per degree increase (or decrease) in temperature.

The test for automatic measurement of the EC was similar to that described above except that no impedances were recorded manually here. Instead, a computer program, using option 3 in the programming instruction 100 of the P208 software of the Campbell Scientific, was downloaded to a datalogger (Campbell Scientific CR10). The value of the probe constant, K_p , was taken as unity in the program so that the datalogger recorded the value of $(1 - \rho_r)/[Z(1 + \rho_r)]$ in Equation 2. The conductivity of the solution was increased step-wise up to 28 dS m^{-1} (18 g l^{-1}). The samples of solution were collected and the temperatures were also recorded at each step. Three sensors of type 1 and five of type 2 (Table 3) were used in this test.

Calibration of the sensors for bulk EC

The constant impedances of the TDR reflectogram after multiple reflections are highly correlated to the electrical conductivities of the solutions. The plot of the reciprocal of the impedances, V_f , against the bulk electrical conductivities, σ , of the solutions is non-linear (Fig. 3). This non-linearity increases with increasing conductivity. All sensors of a particular type show almost the same characteristics except for the second type which contains silicone. The characteristics differ for each sensor of this type (Fig. 3). The measured impedances for all the sensors were interpreted with different non-linear equations. The equations were compared by their coefficients of determination, R^2 . Extra parameters yielding a small increase in R^2 were not retained.

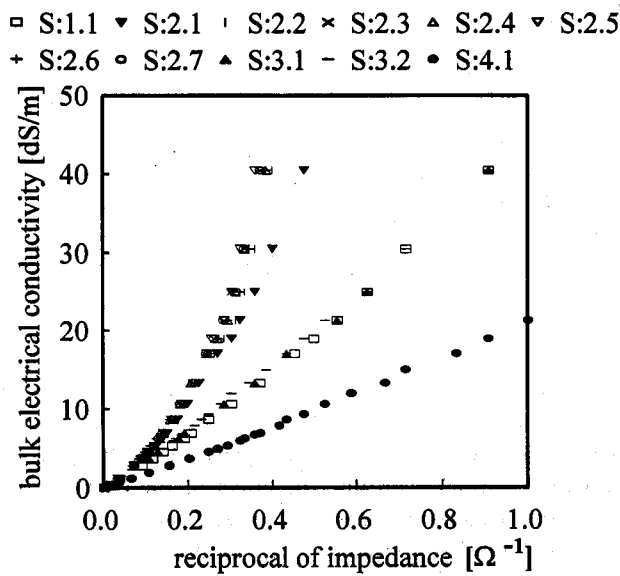


Fig. 3 Relation between impedance of TDR signal and electrical conductivity of salt solution for different sensors.

The electrical conductivities of the solutions and the reciprocal of the impedances are more easily related by polynomial equations of the form:

$$\sigma = A_0 + A_1V_f^{-1} + A_2V_f^{-2} + A_3V_f^{-3} + A_4V_f^{-4} \quad (3)$$

where σ is the electrical conductivity of solutions (S m^{-1}), V_f is the impedance of the TDR signal after multiple reflections (Ω , Fig. 1), and A_0 to A_4 are arbitrary parameters which depend on the characteristics of a specific sensor. Third- and fourth-degree polynomials with zero intercept ($A_0 = 0$) fit the observations very well for all sensors of the first and second type. However, a second-degree polynomial is sufficient to fit the data of the third- and fourth-type sensors. There are no differences among replicate experiments for the same sensor. The polynomial equation (Eq. 3) was fitted separately for the individual sensors of the second type. However, the equation was fitted for all the sensors of the first and third type as a whole since their individual behaviours were almost the same. The impedances measured at 50, 100 and 624 m on the wave form were used separately for all sensors. They showed virtually the same results.

The method proposed by Heimovaara (Eq. 1) was also tested with the experimental data of the second-type sensors. The probe constant, K_p , and the combined series resistance, R_{cs} , in Equation 1 were optimised from the observed data. The electrical conductivities of the solutions were correlated to the quantities recorded by the datalogger. The relation is non-linear and the degree of non-linearity depends on the characteristics of the sensor. However, over the lower range of EC ($<10 \text{ dS m}^{-1}$), the

relation appears to be linear. In this linear region, the probe constant, K_c , was determined for the different sensors by linear regression.

Results and discussion

The seven sensors of the second type containing silicone behaved differently. Over the lower electrical conductivities, the data points followed a linear relation (Fig. 3). But, as the EC increased, the relation became non-linear and the different sensors followed different curves (Fig. 3). Similar results were also observed by Retherford *et al.* (1992) and Heimovaara (1993). However, the structure of the equation (Eq. 3) remained the same for all the sensors and only the parameters (A_0 , A_1 , A_2 , A_3 & A_4) changed. Separate calibration of individual sensors fitted the observations over the whole range (0–44 dS m^{-1}) of the conductivities used in the experiments. The calibration procedure of Heimovaara (1993) also provided a good fit to the measurements. Figure 4 compares the measured and predicted electrical conductivities by the polynomial relation (Eq. 3) and by the method of Heimovaara (Eq. 1) for sensor 2.1 as an example. The method of Heimovaara sometimes overestimated the conductivity over the lower range. The accuracy and degree of fit by the two methods were compared by their coefficients of determination (R^2). Table 4 shows R^2 , combined series resistance, R_{cs} , and probe constant, K_c , estimated by Equation 1. The values of R^2 were very high in both methods and for all sensors. It is evident that the polynomial relations always resulted in higher

▲ measured EC — polynomial estimate
+ Heimovaara estimate

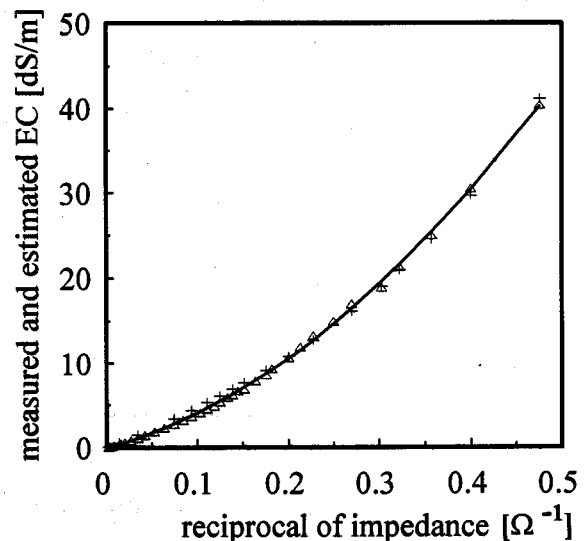


Fig. 4 Fitting of measured electrical conductivity (EC) to calibration functions (Eqs 1 and 3) for sensor 2.1.

Table 4. Coefficient of determination, R^2 , combined series resistance, R_{cs} , and probe constant, K_c , for the seven sensors of type 2

Method	Parameter	Sensor 2.1	Sensor 2.2	Sensor 2.3	Sensor 2.4	Sensor 2.5	Sensor 2.6	Sensor 2.7
Polynomial (Eq. 3)	R^2	0.998	0.999	1.000	0.999	0.999	1.000	0.999
Heimovaara (Eq. 1)	R^2	0.997	0.998	0.999	0.996	0.998	0.998	0.998
	R_{cs} (Ω)	1.064	1.620	1.778	1.623	1.904	1.629	1.760
	K_c (m^{-1})	4.267	3.547	3.744	3.995	3.607	3.881	3.778

values of R^2 (Table 4) than the method of Heimovaara. Because the sensors were tested over a wide range of conductivity ($0 - 44 \text{ dS m}^{-1}$), a small variation in R^2 caused considerable variations in the prediction of the conductivities over the lower range because of smaller conductivities. However, the evidence of higher R^2 by the polynomial equations confirmed the superiority of this method over the other. Although the geometry and the construction materials were the same for the seven sensors, K_c and R_{cs} were governed by the characteristics of the individual sensors (Table 4).

After removing the silicone, the sensors of the second type behaved essentially in the same manner as the first type. The third experiment confirmed this by giving the same calibration equation for sensor types 1 and 2. The estimated ECs for all sensors of the first and second type (after removing the silicone) fitted the observations very well (Fig. 5) with an excellent coefficient of determina-

tion (0.999). This fact implies that the characteristics of the head of the sensor must be taken into account in calibrating sensors to measure EC. Separate calibration of individual sensors overcame the effect of the characteristics of the head of the sensors. A single calibration equation fitted the observed electrical conductivities for the two sensors of the third type with a very high coefficient of determination (0.997). Figure 6 demonstrates the fitting of the observed and estimated ECs for these sensors. The same relation for the data of the fourth-type sensor is shown in Figure 7. The coefficient of determination is again very high ($R^2 = 0.998$).

The calibration functions for all sensors of the four types have been compared in Figure 8. The first- and third-type sensors showed nearly similar behaviour in their performance but the seven sensors of the second type performed differently. The differences were most evident at higher ECs. The first- and second-type sen-

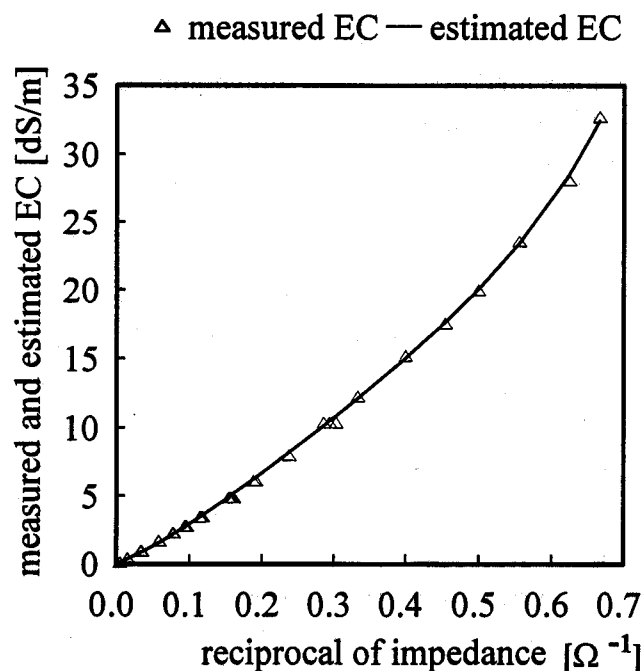


Fig. 5 Fitting of measured electrical conductivity (EC) to calibration function (Eq. 3) for sensors of types 1 and 2 after removing silicone.

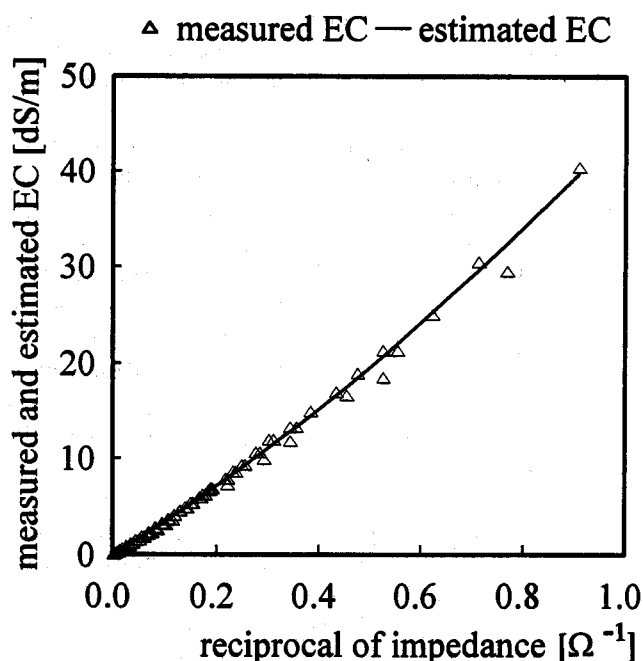


Fig. 6 Fitting of measured electrical conductivity (EC) to calibration function (Eq. 3) for sensors of type 3.

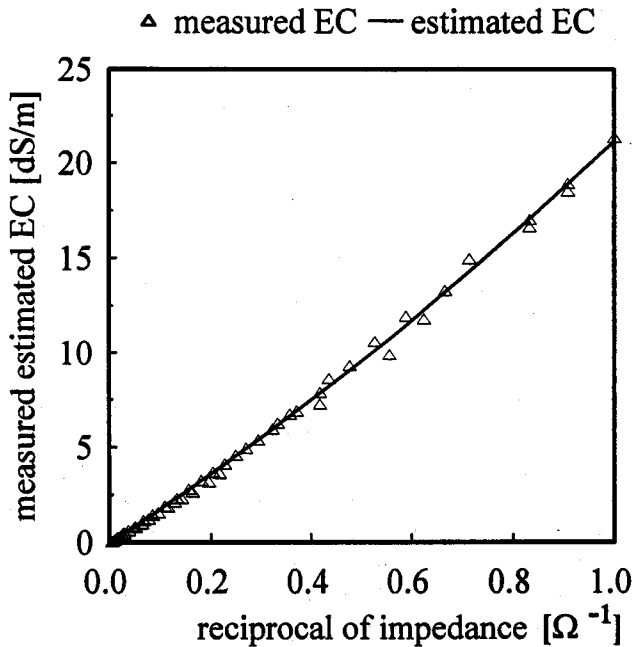


Fig. 7 Fitting of measured electrical conductivity (EC) to calibration function (Eq. 3) for sensors of type 4.

sors had virtually the same geometry. The difference between them was only in the head of the sensor. In the first type, the inside was filled with air ; in the second type, it was filled with silicone which is a good insulator. The energy loss inside the heads of the second-type sensors was less than in the first type. This was demonstrated by the upward shifting of the curves for the second-type sensors (Fig. 8). This energy loss in a TDR sensor, which is proportional to the conductivity of the surrounding medium, is a very important factor in the estimation of ECs from the measurements of impedances. The TDR sends a voltage wave through the coaxial cable connected to the sensor. It measures internally a voltage reflection coefficient, ρ_r , which is the ratio of the voltage reflected from the sensor to that launched through the sensor. The Tektronix 1502C translates the vertical ordinate of the reflected voltage into an equivalent impedance of the signal for a lossless cable. The equivalent impedance, Z_e (Ω), which is proportional to the conductivity of the medium (Eq. 2), is (Anonymous, 1983):

$$Z_e = Z(1 + \rho_r)/(1 - \rho_r) \quad (4)$$

where Z is the impedance of the cable (Ω). For a perfectly lossless cable, the absolute value of the voltage reflection coefficient, ρ_r , is unity. In a short-circuited cable, ρ_r is -1 and the equivalent impedance, Z_e , is zero according to Equation 4. But, in an open circuit, ρ_r is 1 and Z_e is infinite.

The equivalent impedance (Z_e), displayed as V_0 , V_1 , V_2 and V_f on the TDR screen (Fig. 1), is a semi-

quantitative measure of the impedance of the coaxial cable and/or sensor connected to the cable. This is partly because commercial TDR instruments calculate equivalent impedance compared to a reference impedance of a lossless cable. In addition to the simplification by Equation 4 for lossless cables, the attenuation of the travelling pulse is also enhanced by the length of the cable because of its resistance. The Tektronix application note (Anonymous, 1983) clearly warns of this attenuation along the length of the cable: 'Pulse amplitude reduction does not create major problems in locating and identifying cable faults but does make it difficult to measure absolute reflection coefficient at a point some distance down a cable.' The problems of energy loss with the length of the cable, and the fact that Equation 4 is valid only for a lossless medium, are important complications for the measurement of EC by TDR. The sensor in a salt solution or saline soil resembles a wave guide in a lossy medium and is certainly not lossless. Therefore, the measurement of EC by TDR is an approximation.

For low electrical conductivities ($<10 \text{ dS m}^{-1}$), the relation between the ECs and the reciprocal of the impedances appears to be linear (Fig. 3), but the linear relation underestimates electrical conductivities over the lowest range ($<0.5 \text{ dS m}^{-1}$). However, the polynomial relation (Eq. 3) results in an accurate estimation. In addition to this, the correlation improves when the two variables (electrical conductivity and impedance) are correlated by Equation 3. Over higher conductivities, the curvilinearity becomes very distinct and increases with increasing EC (Eq. 3).

- S: 1 ▽ S: 2.1 — S: 2.2 △ S: 2.3 + S: 2.4
- S: 2.5 □ S: 2.6 ▽ S: 2.7 — S: 3 × S: 4

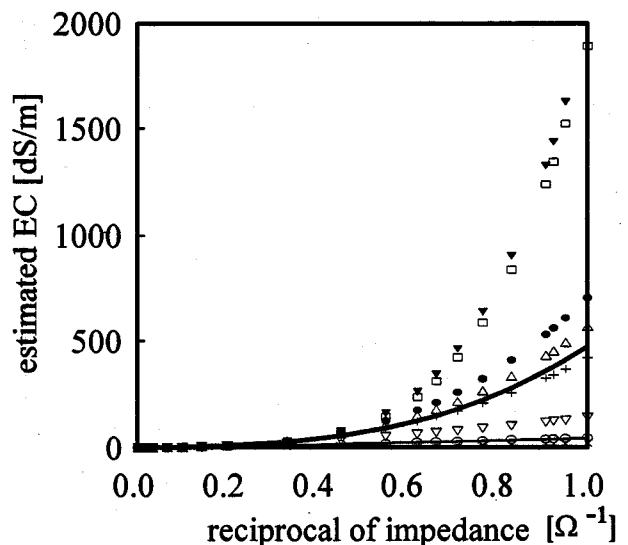


Fig. 8 Comparison of calibration equations for all four types of sensor.

Table 5. Coefficient of determination, R^2 , and probe constant, K_p , for automatic measurement

Method	Parameter	Sensor 1.1	Sensor 1.2	Sensor 1.3	Sensor 2.2	Sensor 2.3	Sensor 2.4	Sensor 2.5	Sensor 2.6
Polynomial(Eq. 3)	R^2	0.990	1.000	0.998	1.000	0.999	0.999	0.993	0.997
Giese and Tiemann (Eq. 2)	R^2	—	0.996	0.992	0.996	0.996	0.997	0.993	0.997
	K_p (m^{-1})	—	3.325	3.607	3.343	3.381	3.394	3.604	3.472

In the case of automatic measurement by a datalogger, the relation between electrical conductivity, σ , and the quantity (the reciprocal of equivalent impedance), $[(1 - \rho_r)/Z(1 + \rho_r)]$ in Equation 2, measured by the datalogger, is found to be non-linear (Fig.9). Therefore, the method of Giese and Tiemann (Eq. 2) cannot predict the observed conductivities in the non-linear region. This is because σ is linearly related to $[(1 - \rho_r)/Z(1 + \rho_r)]$ in Equation 2. However, a second-degree polynomial fits σ and $[(1 - \rho_r)/Z(1 + \rho_r)]$ for all sensors. But, for low values of EC (<10 dS m^{-1}), a linear relation holds and the equation of Giese and Tiemann (Eq. 2) fits the measured data well. Table 5 summarises the coefficients of determination, R^2 , and the probe constant, K_p , for the polynomial and Giese and Tiemann methods. The values of R^2 are reasonably high and indicate the good fitting of the predicted and measured conductivities. The value of K_p varies slightly among the sensors (3.45 ± 0.12 m^{-1}).

The calibration procedures presented here can be used

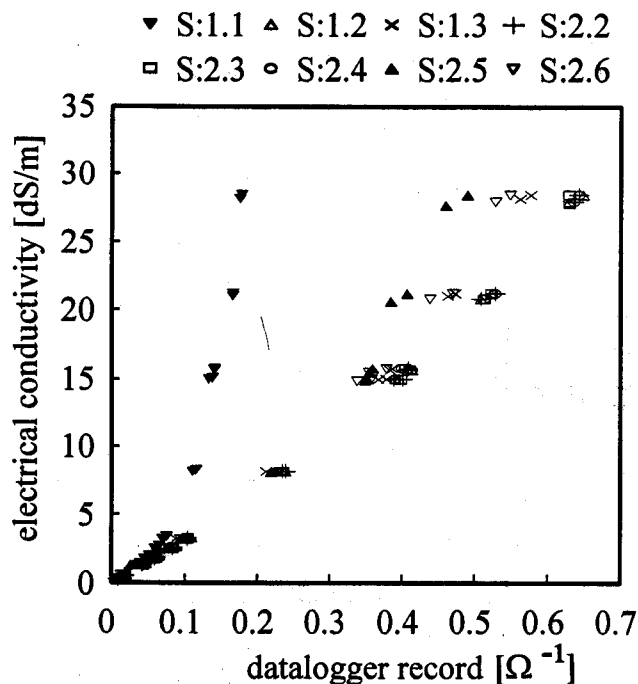


Fig. 9 Relation between $(1 - \rho_r)/[Z(1 + \rho_r)]$ from datalogger records and electrical conductivity, σ , of solution for sensors of types 1 and 2.

successfully to measure a wide range of EC. The highest and lowest values of the impedance measured by TDR are 1000 Ω and 1 Ω , respectively, and consequently the lowest and highest ECs are obtained at 1000 Ω and 1 Ω , respectively. The geometry of the sensors (especially the length of the wire) and the materials used in the head of the sensor affect the attenuation of the TDR signal, and thus determine the range of the measurements. The proposed calibration procedures (polynomial functions) can measure much higher conductivities than those reported by Zegelin *et al.* (1989). However, at very high concentrations of salt (>19 g l^{-1} = 0.33 N NaCl), that is, for conductivities greater than 30 dS m^{-1} , the impedance of the TDR wave becomes less sensitive to σ . The impedance decreases non-linearly at a diminished rate with increasing concentration of salt. At this stage, addition of a small quantity of salt increases σ of the solution, but does not cause any change in the impedance. This affects the accuracy of the measurement at higher ECs (when impedance is less than about 3 Ω). However, these higher conductivities are seldom encountered in practice.

TDR is, thus, able to measure a wide range of EC using a parallel three-wire sensor. This can measure ECs of a solution and also of a soil-water system. The sensor needs to be calibrated first in salt solution to establish the governing equation. The equation is simple and needs only one measurement of the impedance on the TDR trace for the manual measurement. The automatic measurement is much simpler than manual measurements. This calibration technique opens a new perspective to measure electrical conductivity by TDR.

Acknowledgements

During this work, Dr M.A. Mojid held a Commonwealth Scholarship and was on leave from Bangladesh Agricultural University, Mymensingh, Bangladesh.

References

- Anonymous, 1983. TDR for cable testing. Application note AX-3241-1, Tektronix Inc., Beaverton, OR97077, USA.
- Dalton, F.N., 1992. Development of time-domain reflectometry for measuring soil water content and bulk soil electrical conductivity. In: G.C. Topp, W.D. Reynolds and R.E. Green

- (Editors), *Advances in Measurement of Soil Physical Properties: Bringing Theory into Practice*. Soil Science Society of America, Madison, WI, Special Publication No. 30, pp. 143–167.
- Dalton, F.N. and van Genuchten, M.Th., 1986. The time-domain reflectometry method for measuring soil water content and salinity. *Geoderma*, **38**: 237–250.
- Dalton, F.N., Herkelrath, W.N., Rawlins, D.S. and Rhoades, J.D., 1984. Time-domain reflectometry: simultaneous measurement of soil water content and electrical conductivity with a single probe. *Science*, **224**: 989–990.
- Giese, K. and Tiemann, R., 1975. Determination of the complex permittivity from thin-sample time-domain reflectometry. Improved analysis of the step response wave form. *Adv. Mol. Relax. Processes*, **7**: 45–59.
- Heimovaara, T.J., 1993. Design of triple-wire time-domain reflectometry probes in practice and theory. *Soil Sci. Soc. Am. J.*, **57**: 1410–1417.
- Kachanoski, R.G., Pringle, E. and Ward, A.L., 1992. Field measurement of solute travel times using time-domain reflectometry. *Soil Sci. Soc. Am. J.*, **56**: 47–52.
- Kraus, J.D., 1992. *Electromagnetics* (4th ed.). McGraw-Hill, New York.
- Mallants, D., Vanclooster, M., Meddahi, M. and Feyen, J., 1994. Estimating solute transport in undisturbed soil columns using time-domain reflectometry. *J. Contam. Hydrol.*, **5**: 91–109.
- Mallants, D., Vanclooster, M., Toride, N., Vanderborght, J., van Genuchten, M.Th. and Feyen, J., 1996. Comparison of three methods to calibrate TDR for monitoring solute movement in unsaturated soil. *Soil Sci. Soc. Am. J.*, **60**: 747–754.
- Mojid, M.A., 1996. Use of time-domain reflectometry to measure water content and solute-transport parameters in unsaturated soils. Ph.D. thesis, University of Newcastle upon Tyne, UK, 237 pp.
- Nadler, A., Dasberg, S. and Lapid, I., 1991. Time-domain reflectometry measurements of water content and electrical conductivity of layered soil columns. *Soil Sci. Soc. Am. J.*, **55**: 938–943.
- Retherford, C.A., Hamlett, J.M. and Morrow, C.T., 1992. Greenhouse container water content and electrical conductivity measurement. *Trans. ASAE*, No. 92-2554.
- Topp, G.C., Yanuka, M., Zebchuk, W.D. and Zegelin, S., 1988. Determination of electrical conductivity using time-domain reflectometry: soil and water experiments in coaxial lines. *Wat. Resour. Res.*, **24**: 945–952.
- Vancllooster, M., Mallants, D., Diels, J. and Feyen, J., 1993. Determining local-scale solute transport parameters using time-domain reflectometry (TDR). *J. Hydrol.*, **148**: 93–107.
- Vancllooster, M., Gonzalez, C., Vanderborght, J., Mallants, D. and Diels, J., 1994. An indirect calibration procedure for using TDR in solute transport studies. US Department of Interior Bureau of Mines, Special publication SP 19-94.
- Vancllooster, M., Mallants, D., Vanderborght, J., Diels, J., Van Orshoven, J. and Feyen, J., 1995. Monitoring solute transport in a multi-layered sandy lysimeter using time-domain reflectometry. *Soil Sci. Soc. Am. J.*, **59**: 337–344.
- Vogeler, I., Clothier, B.E., Green, S.R., Scotter, D.R. and Tillman, R.W., 1996. Characterising water and solute movement by time-domain reflectometry and disk permeametry. *Soil Sci. Soc. Am. J.*, **60**: 5–12.
- Ward, A.L., Kachanoski, R.G. and Elrick, D.E., 1994. Laboratory measurements of solute transport using time-domain reflectometry. *Soil Sci. Soc. Am. J.*, **58**: 1031–1039.
- Ward, A.L., Kachanoski, R.G., von Bertoldi, A.P. and Elrick, D.E., 1995. Field and undisturbed-column measurements for predicting transport in unsaturated layered soil. *Soil Sci. Soc. Am. J.*, **59**: 52–59.
- Yanuka, M., Topp, G.C., Zegelin, S. and Zebchuk, W.D., 1988. Multiple reflection and attenuation of time-domain reflectometry pulses: theoretical considerations for applications to soil water. *Wat. Resour. Res.*, **24**: 939–944.
- Zegelin, S.J., White, I. and Jenkins, D.R., 1989. Improved field probes for soil water content and electrical conductivity measurement using time-domain reflectometry. *Wat. Resour. Res.*, **25**: 2367–2376.